

# Conformation-Dependent $^{13}\text{C}$ NMR Chemical Shifts of Poly(L-alanine) in the Solid State: FPT INDO Calculation of *N*-Acetyl-*N'*-methyl-L-alanine Amide as a Model Compound of Poly(L-alanine)

Isao Ando,\*† Hazime Saitô,† Ryoko Tabeta,† Akira Shoji,§ and Takuo Ozaki§

Department of Polymer Chemistry, Tokyo Institute of Technology, Ookayama, Meguro-ku, Tokyo, Japan 152, Biophysics Division, National Cancer Center Research Institute, Tsukiji, Chuo-ku, Tokyo, Japan 104, and Department of Industrial Chemistry, College of Technology, Gunma University, Tenjin-cho, Kiryu-shi, Gunma, Japan 376.  
Received February 14, 1983

**ABSTRACT:** An attempt is made to calculate  $^{13}\text{C}$  NMR chemical shifts of *N*-acetyl-*N'*-methyl-L-alanine amide, a model compound for poly(L-alanine), as functions of the dihedral angles  $\phi$  and  $\psi$  specifying the peptide chain, by using the FPT INDO method, in order to obtain a clue as to the origin of the conformation-dependent  $^{13}\text{C}$  NMR chemical shift previously determined for solid oligo(L-alanines) and poly(L-alanine), and copolymers of L- and D-alanines by the cross-polarization/magic angle spinning technique. It is found that the calculated results on  $\text{C}_\alpha$ ,  $\text{C}_\beta$ , and carbonyl carbons exhibit conformation-dependent  $^{13}\text{C}$  chemical shifts comparable with the experimental data.

## Introduction

Recent  $^{13}\text{C}$  NMR studies of solid polypeptides,<sup>1-3</sup> as measured by the cross-polarization/magic angle spinning (CP/MAS) technique,<sup>4,5</sup> demonstrated that  $^{13}\text{C}$  NMR chemical shifts of the  $\text{C}_\alpha$ ,  $\text{C}_\beta$ , and carbonyl carbons are considerably displaced, up to 7 ppm, depending on the particular conformations adopted, such as  $\alpha$ -helix and  $\beta$ -sheet forms. The existence of such conformation-dependent  $^{13}\text{C}$  chemical shifts is very valuable in examining whether or not the conformation of the polypeptide under consideration is retained in the solution state. This approach can be extended to probe local conformations of amino acids in peptides<sup>6,7</sup> and proteins<sup>8,9</sup> by taking into account the finding that  $^{13}\text{C}$  chemical shifts of an amino acid residue in random coil conformation are effectively independent of the neighbors except for the presence of proline residues.<sup>10</sup>

It is reasonable to ascribe conformation-dependent  $^{13}\text{C}$  chemical shifts to changes of electronic structure accompanying changes of the dihedral angles of the skeletal peptide bonds. To prove this view, we attempted to calculate relative  $^{13}\text{C}$  chemical shifts of a dipeptide fragment of poly(L-alanine),<sup>11</sup> *N*-acetyl-*N'*-methyl-L-alanine amide, employing the finite perturbation INDO (FPT INDO) theory.<sup>15,16</sup> It is sufficient to employ such a dipeptide fragment in the elucidation of the chemical shift behavior of poly(L-alanine) and oligo(L-alanines), and copolymers of L- and D-alanines because the chemical shift is sensitive in most cases to the local structure. Such an attempt, therefore, is valuable in understanding the origin of  $^{13}\text{C}$  chemical shifts as well as in providing insight into  $^{13}\text{C}$  chemical shifts of unstable conformers which are experimentally unattainable.<sup>12,17</sup>

## Theoretical Section

The magnetic shielding,  $\sigma^A$ , of nucleus A in a molecule with atoms A, B, and others may be written as<sup>16</sup>

$$\sigma^A = \sigma_d^{AA} + \sigma_p^{AA} + \sum_{B(\neq A)} \sigma^{AB} \quad (1)$$

where  $\sigma_d^{AA}$  and  $\sigma_p^{AA}$  are the local diamagnetic and paramagnetic terms, respectively, and  $\sigma^{AB}$  is the contribution

from the remaining atoms. The dominant factor usually governing  $^{13}\text{C}$  chemical shifts is  $\sigma_d^{AA}$ , whereas  $\sigma_d^{AB}$  makes only a small contribution and  $\sigma_p^{AB}$  may be negligible because it is unlikely to exceed a few parts per million.

The FPT INDO theory has the advantage of permitting the calculation of the paramagnetic term without the use of the explicit wave function for excited states, which cannot be obtained accurately by an ordinary SCF MO theory. For this reason, the FPT INDO theory has successfully explained the  $^{13}\text{C}$  chemical shifts of various organic compounds.<sup>18</sup> According to the FPT INDO theory,<sup>15,16</sup>  $\sigma_d^{AA}$  and  $\sigma_p^{AA}$  are expressed by

$$\sigma_d^{AA} = \frac{1}{3} \frac{e^2}{2mc} \sum_{\beta} \sum_{\mu} \sum_{\nu} P_{\mu\nu}(0) \left\langle \chi_{\nu} \left| \frac{\mathbf{r}_{\nu} \mathbf{r}_A - r_{\nu A} \mathbf{r}_A}{|\mathbf{r}_A|^3} \right| \chi_{\nu} \right\rangle \quad (2)$$

$$\sigma_p^{AA} = -\frac{1}{3} \frac{e\hbar}{mc} i \sum_{\beta} \sum_{\mu} \sum_{\nu} \left( \frac{\partial P_{\mu\nu}(\mathbf{H}_A)}{\partial \mathbf{H}_A} \right)_{\mathbf{H}=0} \left\langle \chi_{\mu} \left| \frac{(\mathbf{r} \times \nabla)_{\beta}}{|\mathbf{r}_A|^3} \right| \chi_{\nu} \right\rangle \quad (3)$$

$\alpha, \beta = x, y, z$

where the gauge origin of the vector potential is set at the position of nucleus A. The vectors  $\mathbf{r}_{\nu}$  and  $\mathbf{r}_A$  are the position vectors of an electron considered from a nucleus of the atom containing the atomic orbital  $\chi_{\nu}$  and from the nucleus A, respectively.  $P_{\mu\nu}(\mathbf{H}_A)$  and  $P_{\mu\nu}(0)$  are the elements of the density matrix with and without the perturbation due to the magnetic field,  $\mathbf{H}$ , respectively. These are obtained by solving the Roothaan equation with the Hartree-Fock matrix,  $F_{\mu\nu}(\mathbf{H}_A)$ , containing the perturbation terms in the INDO framework.

$$F_{\mu\nu}(\mathbf{H}_A) = \mathcal{H}_{\mu\nu}^{\text{core}} + \sum_{\lambda} \sum_{\sigma} P_{\lambda\sigma}(\mathbf{H}_A) \left\{ (\mu\nu|\lambda\sigma) - \frac{1}{2} (\mu\sigma|\lambda\nu) \right\} - i \left( \frac{e\hbar}{2mc} \right) \sum_{\alpha} H_{\alpha} \langle \chi_{\mu} | (\mathbf{r} \times \nabla)_{\alpha} | \chi_{\nu} \rangle \quad (4)$$

In this equation, the first two terms on the right-hand side are the ordinary Hartree-Fock matrix and the last term is the perturbation due to the magnetic field, which is given as an imaginary number.  $\mathcal{H}_{\mu\nu}^{\text{core}}$ ,  $(\mu\nu|\lambda\sigma)$ , and  $(\mu\sigma|\lambda\nu)$  are the unperturbed core Hamiltonian, Coulomb integral, and exchange integral, respectively. These are estimated by parameters within the INDO framework. In the present work, we shall adopt Pople's parameter in the INDO

\* Tokyo Institute of Technology.

† National Cancer Center Research Institute.

§ Gunma University.

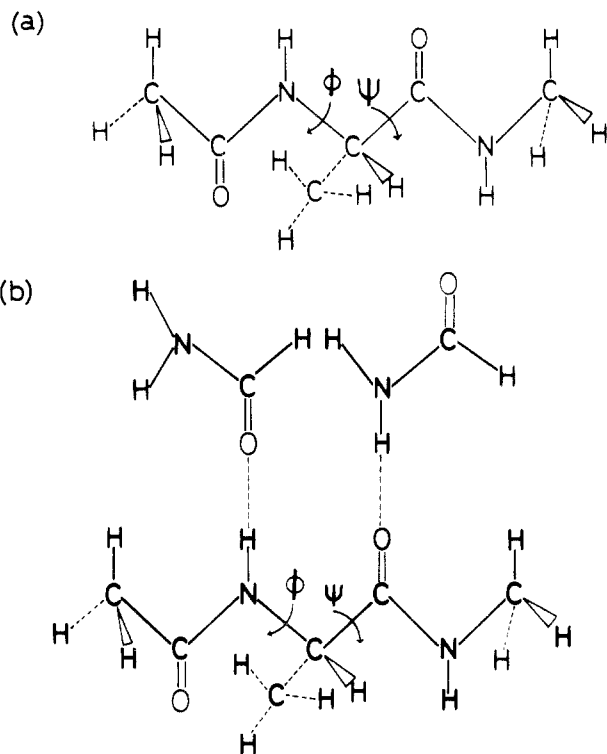


**Figure 1.** The molecular structure of *N*-acetyl-*N'*-methyl-L-alanine amide: (a) model I; (b) model II (taking hydrogen bonds with two formamide molecules),  $\phi = \psi = 180^\circ$ .

method except for the off-diagonal element of the core Hamiltonian, which is estimated from the expression

$$\mathcal{H}_{\mu\nu}^{\text{core}} = (\kappa_\pi/2)(\beta^\circ_A + \beta^\circ_B)S_{\mu\nu} \quad (5)$$

in which  $\kappa_\pi$  denotes a correlation factor for the  $\pi$ - $\pi$  interaction,  $\beta^\circ_A$  the bonding parameter for atom A, and  $S_{\mu\nu}$  the overlap integral. In the present calculation, a parameter set which reproduces fairly well the  $^{13}\text{C}$  chemical shift of hydrocarbons was used:  $\beta^\circ_{\text{H}} = -13$  eV,  $\beta^\circ_{\text{C}} = -15$  eV,  $\beta^\circ_{\text{N}} = -25$  eV, and  $\beta^\circ_{\text{O}} = -31$  eV for hydrogen, carbon, nitrogen, and oxygen atoms, respectively.<sup>16</sup>

The differential coefficient in eq 3 is replaced numerically by

$$\left( \frac{\partial P_{\mu\nu}(\mathbf{H}_\alpha)}{\partial \mathbf{H}_\alpha} \right)_{\mathbf{H}=0} = \text{Im} (P_{\mu\nu}(\mathbf{H}_\alpha)) / \mathbf{H}_\alpha \quad (6)$$

where  $\text{Im} (P_{\mu\nu}(\mathbf{H}_\alpha))$  denotes the imaginary part of the density matrix  $P_{\mu\nu}(\mathbf{H}_\alpha)$ . These molecular integrals were evaluated by means of the Gaussian-transform method presented by Karplus et al.<sup>19</sup>

We adopted the molecular geometry of *N*-acetyl-*N'*-methyl-L-alanine amide from the values proposed by Momany et al.<sup>20</sup> For the calculation, the dihedral angles  $\phi$  and  $\psi$  (Figure 1) are varied at  $15^\circ$  intervals. It appears obvious that this calculation (model I) may not be good enough for the  $\text{C}_\alpha$  and carbonyl carbons, because the intramolecular and intermolecular hydrogen bonds for the  $\alpha$ -helix and  $\beta$ -sheet forms, respectively, might strongly affect the chemical shifts of these carbons. Thus, we performed an alternative calculation on a model system (model II) in which two formamides are hydrogen bonded to the amide groups of the dipeptide in an appropriate geometry with the  $\alpha$ -helix and  $\beta$ -sheet forms (Figure 1). The structural data, including the distance between nitrogen and oxygen atoms, 2.83 and 2.87 Å for the  $\beta$ -sheet and  $\alpha$ -helix forms, respectively, were taken from X-ray diffraction studies of poly(L-alanines) by Arnott et al.<sup>21,22</sup>

The chemical shift,  $\delta^{\text{coil}}$ , for the random-coil conformation is related to the mole fraction  $p_i$  and the characteristic chemical shift,  $\delta_i$ , of individual preferred conformers by

$$\delta^{\text{coil}} = \sum_i p_i \delta_i \quad (7)$$

The calculation for  $\delta^{\text{coil}}$  was carried out by the averaging of  $\delta^{\text{coil}}$  with  $p_i$ , which is computed from the total energy of conformer  $i$  obtained from the INDO calculation.

HITAC M 200H computers at the Computer Center of the Tokyo Institute of Technology and at the Computer Center of the Institute for Molecular Science were used for the calculation.

## Results and Discussion

**$^{13}\text{C}$  Chemical Shifts of (Ala) $_n$ .** Figure 2 shows the  $^{13}\text{C}$  chemical shift contour map of the  $\text{C}_\alpha$ ,  $\text{C}_\beta$ , and carbonyl carbons of *N*-acetyl-*N'*-methyl-L-alanine amide for model I, calculated by the FPT INDO theory, as a function of the dihedral angles  $\phi$  and  $\psi$  whose values were varied in  $15^\circ$  intervals. The chemical shift is expressed in ppm, which was interpolated from the calculation at  $15^\circ$  intervals. The right-handed and left-handed  $\alpha$ -helix ( $\alpha_R$  and  $\alpha_L$ , respectively) regions, and the antiparallel and parallel  $\beta$ -sheet ( $\beta_A$  and  $\beta_P$ , respectively) regions are indicated by solid circle, as deduced from X-ray studies made on poly(L-alanine).<sup>21,22</sup>

We first consider the contour map for the  $\text{C}_\beta$  carbon (Figure 2a), because the chemical shift of the  $\text{C}_\beta$  carbon is not strongly affected by the formation of a hydrogen bond, as described below. The chemical shift in the  $\alpha_R$ -helix form appears at higher field than that in the  $\alpha_L$ -helix form, and the variation of the chemical shift with the dihedral angles  $\phi$  and  $\psi$  in the vicinity of the former is larger than that of the latter. On the other hand, both the positions for the  $\beta_A$ - and  $\beta_P$ -sheet forms fall on the same contour, so their chemical shifts are nearly equal. Thus, the chemical shifts for  $\beta_A$ - and  $\beta_P$ -sheet forms appear at lower field than those in the  $\alpha$ -helix forms and  $\beta_A$ - and  $\beta_P$ -sheet forms cannot be distinguished from each other by the chemical shifts for the  $\text{C}_\beta$  carbon. The numerical values of the  $^{13}\text{C}$  chemical shifts of  $\alpha_R$ - and  $\alpha_L$ -helix forms, and  $\beta_A$ - and  $\beta_P$ -sheet forms are summarized in Table I.

Next, we consider the contour maps for the  $\text{C}_\alpha$  and carbonyl carbons (Figure 2b,c). It appears, as far as the  $\text{C}_\alpha$  carbon is concerned, that the chemical shift for the  $\alpha_R$  form is at lower field than that for the  $\alpha_L$  form (the difference between them being about 1 ppm) and there is also a significant displacement between the  $\beta_A$  and  $\beta_P$  forms, in contrast to the case of the  $\text{C}_\beta$  carbon. Accordingly, the  $\beta_A$ - and  $\beta_P$ -sheet structures could be distinguished through the chemical shift of the  $\text{C}_\alpha$  carbon. On the other hand, the contour map for the carbonyl carbon shows that the chemical shift for the  $\alpha_R$ -helix form appears at lower field than that for the  $\alpha_L$  form and is at higher field than those for  $\beta_A$ - and  $\beta_P$ -sheet forms. Further, the chemical shift for the  $\beta_A$ -sheet form appears at lower field than that for the  $\beta_P$ -sheet form. Although some features of the contour maps for the  $\text{C}_\alpha$  and carbonyl carbons have been described, there appears to be, as already suggested above, a limitation in the application of the maps to solid poly(L-alanine) because no hydrogen bonding is taken into account. For the sake of comparison, we summarize pertinent numerical values in Table I. In addition, the chemical shifts for the random coil, occurring in solution, were also estimated on the basis of the treatment of eq 7 by using the above contour maps and the total energy (Table I).

As an alternative model which takes into account hydrogen bonding in the  $\alpha$ -helix and  $\beta$ -sheet, we performed numerical calculation of chemical shifts on the basis of

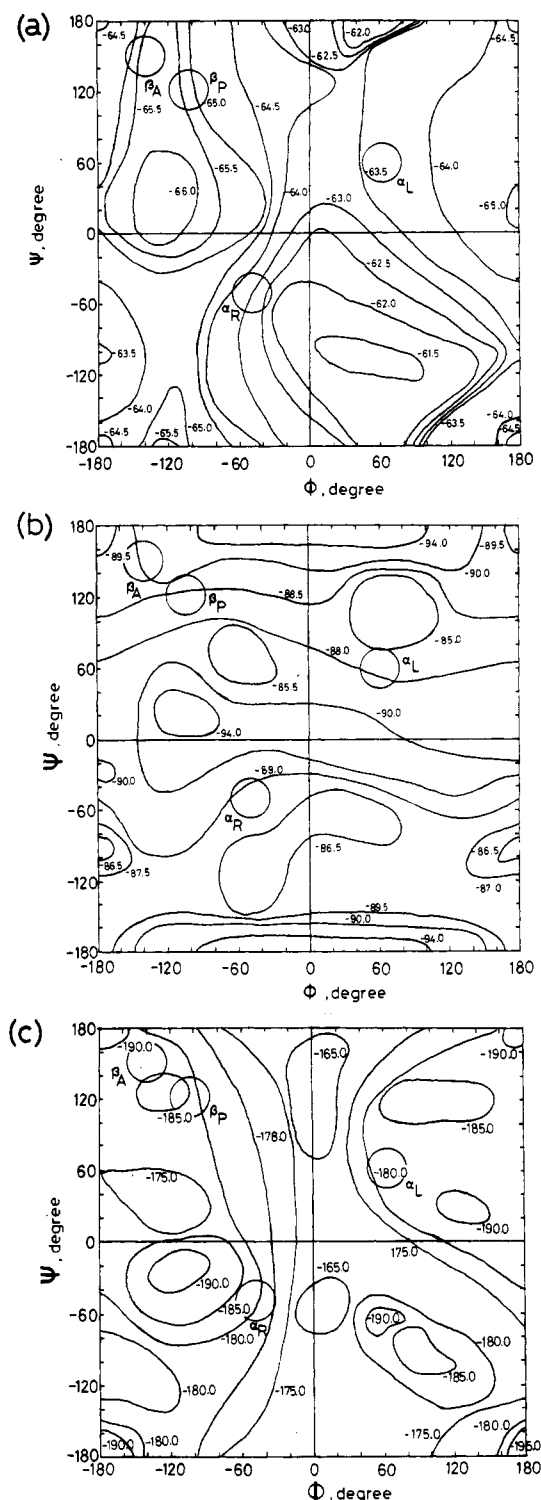


**Figure 2.** The calculated  $^{13}\text{C}$  chemical shift contour maps for the  $\text{C}_\beta$  (a),  $\text{C}_\alpha$  (b), and carbonyl carbons (c) in *N*-acetyl-*N'*-methyl-L-alanine amide. The methyl end groups were held fixed as shown in Figure 1. The chemical shifts were calculated at  $15^\circ$  intervals in  $\phi$  and  $\psi$ .

model II (Table I). It is found that hydrogen bonding leads to an upfield shift for the  $\text{C}_\alpha$  and carbonyl carbon but does not effectively change the chemical shift of the  $\text{C}_\beta$  carbon.

To assist comparison with the experimental data, we reproduce some  $^{13}\text{C}$  NMR spectra taken in the solid state.<sup>3</sup> It is seen from Figure 3A,B and Table I that the calculated chemical shifts of the  $\text{C}_\beta$  carbon on the basis of model I are paralleled by the experimental data in the case of the  $\alpha_R$ -helix,  $\beta_A$ -sheet, and random coil (in trifluoroacetic acid solution) forms in poly(L-alanine)'s while those of the  $\text{C}_\alpha$

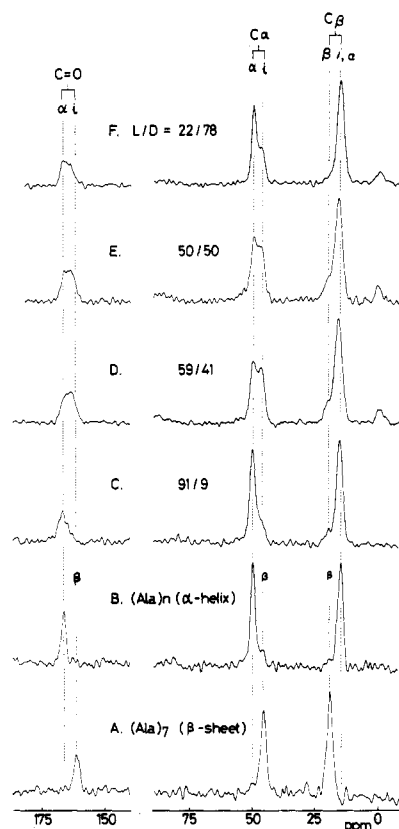


**Figure 3.**  $^{13}\text{C}$  CP/MAS NMR (75.46 MHz) spectra of random copolymers of L-alanine and D-alanine, and poly(L-alanine) in solid state: (A)  $(\text{Ala})_7$ ; (B)  $(\text{Ala})_n$  ( $n = 2800$ ), (C) copolymer  $L/D = 91/9$ ; (D) copolymer  $L/D = 59/41$ ; (E) copolymer  $L/D = 50/50$ ; (F) copolymer  $L/D = 22/78$ . These spectra were reorganized with use of the method published in ref 3. For the experimental conditions see ref 3.

and carbonyl carbons are not. (It is known from X-ray diffraction study that the  $\beta$ -sheet form of poly(L-alanine) has antiparallel.<sup>21,22</sup>) In particular, the difference in chemical shift of the  $\text{C}_\beta$  carbon between the  $\alpha_R$ -helix and  $\beta_A$ -sheet forms is 2.6 ppm, in good agreement with the experimental finding of 5.0 ppm. In addition, the chemical shift of the random coil lies between those of the  $\alpha_R$ -helix and  $\beta_A$ -sheet forms. Therefore, it is clear that the chemical shifts of the  $\text{C}_\beta$  carbon can be mainly explained in terms of the conformational change.

However, the calculated chemical shifts of  $\text{C}_\alpha$  and carbonyl carbons on the basis of model I conflict with the experimental data. It appears that the cause of such disagreement is mainly our choice of model I, neglecting the hydrogen bonding at the amide group, which plays an important role in stabilizing these forms. As shown in Table I, the results of model II show that the formation of the hydrogen bonds at the amide groups causes an upfield displacement for both the carbonyl and  $\text{C}_\alpha$  carbons. Such an effect is more significant for the  $\beta_A$ -sheet form than for the  $\alpha_R$ -helix form (Table I), because in these hydrogen bonds the distance between the nitrogen and oxygen atoms is reported to be shorter for the latter.<sup>21,22</sup> Thus, the difference in the calculated chemical shifts between the  $\alpha_R$ -helix and  $\beta_A$ -sheet forms is 1.6 and 2.1 ppm for the  $\text{C}_\alpha$  and carbonyl carbons, respectively, and is in agreement with the experimental values (4.2 and 4.6 ppm, respectively). Inclusion of the hydrogen bond does not affect the nuclear shielding on the  $\text{C}_\beta$  carbon (slightly downfield shift by 0.1 ppm).

**Application of the Contour Map to the Elucidation of the Conformational Behaviour of Random Co-**

Table I  
<sup>13</sup>C Chemical Shifts of Alanine Peptides Characteristic of  $\alpha$ -Helix,  $\beta$ -Sheet, and Random Coil Forms (in ppm)

obsd <sup>a</sup> (poly(L-alanine))				calcd <sup>b</sup>					
carbon	$\alpha$ -helix	$\beta$ -sheet	random coil <sup>c</sup>	model	$\alpha$ -helix		$\beta$ -sheet		random coil
					$\alpha_R$	$\alpha_L$	$\beta_A$	$\beta_P$	
C $_{\beta}$	14.9	19.9	15.7	I	-63.0	-63.7	-65.6	-65.3	-64.3
				II	-63.1	-63.6	-64.7	-65.4	-63.2 <sup>d</sup>
C $_{\alpha}$	52.4	48.2	51.1	I	-88.5	-88.1	-89.2	-88.2	-87.7
				II	-87.8	-86.4	-86.2	-85.5	-86.9 <sup>d</sup>
CO	176.4	171.8	176.1	I	-184.2	-182.2	-185.7	-185.1	-185.2
				II	-183.1	-181.7	-181.0	-185.6	-182.3 <sup>d</sup>

<sup>a</sup> From tetramethylsilane. Reference 3. <sup>b</sup> Shielding constant for *N*-acetyl-*N'*-methyl-L-alanine amide. <sup>c</sup> In CF<sub>3</sub>COOD solution. <sup>d</sup> Averaged over  $\alpha_R$ ,  $\alpha_L$ ,  $\beta_A$ , and  $\beta_P$  forms.

**polymers of L- and D-Alanines.** In our previous work<sup>3</sup>, we have reported that when the proportion of L-alanine (or D-alanine) is increased in random copolymers of L- and D-alanine, additional peaks (marked by i) appear besides the C=O and C $\alpha$  signals of the  $\alpha_R$ -helix form (marked by  $\alpha$ ). It appears, however, that such a change is not seen in the C $\beta$  signal region. It is plausible that the additional peak in this case is accidentally superimposed on the  $\alpha$ -helical C $\beta$  signal. The anomaly of the distribution of the peak intensities previously mentioned<sup>3</sup> is easily resolved by this new assignment. In parallel with this finding by the CP/MAS data, we found that two peaks of far-infrared spectra (spectra not shown), 420 and 478 cm<sup>-1</sup>, are increased at the expense of the  $\alpha$ -helix peaks (374 and 526 cm<sup>-1</sup>) when the proportion of L- or D-alanine residues in the copolymers is increased. In addition, the peak intensity of the characteristic band of the  $\beta_A$ -sheet (442 cm<sup>-1</sup>) was less than 5–10% of the new peaks mentioned above. This observation is in good agreement with that by Itoh et al.<sup>23</sup> They established the assignment of the infrared peaks (420 and 478 cm<sup>-1</sup>) to D-alanine residues incorporated into the right-handed  $\alpha$ -helix or L-alanine residues in the left-handed  $\alpha$ -helix residues. On the basis of the infrared data, it is now clear to assign the peaks i of the CP/MAS spectra to the L- or D-alanine residues incorporated into the left- or right-handed  $\alpha$ -helices, respectively, in spite of the similarity of the peak positions to the  $\beta$ -sheet form (C=O and C $\alpha$  region).<sup>24</sup>

It is worthwhile to examine whether such an assignment is justified or not on the basis of the contour map as a test of the usefulness of this approach. The  $\alpha_R$ -helix form in poly(L-alanine) and the  $\alpha_L$ -helix form in poly(D-alanine) lie at the same position ( $\alpha_R$ ) in the contour maps where  $\phi = -48^\circ$  and  $\psi = -57^\circ$ .<sup>21,22,25</sup> On the other hand, the D-alanine residues incorporated into the  $\alpha_R$ -helix in a L-alanine sequence or L-alanine residues into the  $\alpha_L$ -helix in a D-alanine sequence lie on the same position ( $\alpha_L$ ) in the contour maps where  $\phi = 48^\circ$  and  $\psi = 57^\circ$ .<sup>23</sup> The chemical shifts of the C $\beta$  carbon in the  $\alpha_L$ -helix appear at the same field as in the  $\alpha_R$ -helix, whereas those of the C $\alpha$  and carbonyl carbons in the  $\alpha_L$ -helix appear at higher field than in the  $\alpha_R$ -helix. The chemical shifts of the C $\alpha$  and carbonyl carbons in the  $\alpha_L$ -helix shift in the direction of the  $\beta_A$ -sheet form (Figure 2 and Table I). These trends are more pronounced when the hydrogen bond is taken into account. The peaks i of the C=O and C $\alpha$  region thus should be at positions very close to those of the  $\beta$ -sheet form, in good agreement with the experimental finding. Downfield displacement of the C $\beta$  signal in the D- or L-alanine residues incorporated into the  $\alpha_R$ -helix is rather small compared with those of the C $\alpha$  and C=O region (Table I), resulting in the overlap with the original C $\beta$  signal. This trend is again consistent with our experimental finding. We find that the calculation of the contour map is very useful as

a means of demonstrating the presence of the D-alanine residues incorporated into the  $\alpha_R$ -helix in an L-alanine sequence or of L-alanine residues incorporated into the  $\alpha_L$ -helix in a D-alanine sequence ( $\phi = 48^\circ$  and  $\psi = 57^\circ$ ), as shown from the <sup>13</sup>C chemical shift values.

In conclusion, we have shown that conformation-dependent <sup>13</sup>C chemical shifts of poly(L-alanines) may be mainly interpreted in terms of the change of the electronic structure brought about by changes in the dihedral angles of the skeletal bonds and also by the intra- or interchain hydrogen bonds.

**Registry No.** *N*-Acetyl-*N'*-methyl-L-alanine amide, 19701-83-8; poly(L-alanine) (homopolymer), 25191-17-7; poly(L-alanine) (SRU), 25213-34-7.

## References and Notes

- (1) T. Taki, S. Yamashita, M. Satoh, A. Shibata, T. Yamashita, R. Tabeta, and H. Saitō, *Chem. Lett.*, 1903 (1981).
- (2) D. Muller and H. R. Kricheldorf, *Polym. Bull.*, **6**, 101 (1981).
- (3) H. Saitō, R. Tabeta, A. Shoji, T. Ozaki, and I. Ando, *Macromolecules*, **16**, 1050 (1983).
- (4) J. Schaefer and E. O. Stejskal in "Topics in Carbon-13 NMR Spectroscopy", G. C. Levy, Ed., Vol. 3, Wiley-Interscience, New York, 1979, p. 283.
- (5) J. R. Lyerla in "Contemporary Topics in Polymer Science", M. Shen, Ed., Vol. 3, Plenum Press, New York, 1979, p. 143.
- (6) L. G. Pease, M. H. Frey, and S. J. Opella, *J. Am. Chem. Soc.*, **103**, 467 (1981).
- (7) L. M. Gierasch, M. H. Frey, J. G. Hexem, and S. J. Opella, *ACS Symp. Ser.*, No. 191, 233 (1982).
- (8) H. Saitō, M. Kameyama, M. Kodama, and C. Nagata, *J. Biochem. (Tokyo)*, **92**, 233 (1982).
- (9) H. Saitō, Y. Iwanaga, R. Tabeta, M. Narita, and T. Asakura, *Chem. Lett.*, 427 (1983).
- (10) O. W. Howarth and D. M. J. Lilley, *Prog. Nucl. Magn. Reson. Spectrosc.*, **12**, 1 (1978).
- (11) Previously, Tonelli<sup>12</sup> explained the variation of <sup>13</sup>C chemical shifts of various peptides in solution in terms of the gauche  $\gamma$ -effect arising from the interaction with the substituent in the  $\gamma$  position.<sup>13,14</sup> For the interpretation of <sup>13</sup>C chemical shifts by this concept, the dipeptide fragment used here may not be large enough to describe the conformation-dependent <sup>13</sup>C chemical shifts of the carbonyl carbons. However, our view is that <sup>13</sup>C chemical shifts are determined by the electronic structure of the conformer under consideration, which is a function of the dihedral angle ( $\phi$  and  $\psi$ ) as well as hydrogen bonds between NH and C=O groups. At present, it is not clear whether the gauche  $\gamma$ -effect arises from the conformational effect or a nonbonded through-space effect or both. If the former is dominant, it is possible to obtain the conformation-dependent <sup>13</sup>C chemical shifts even in the dipeptide fragment, including the term corresponding to the gauche  $\gamma$ -effect. Quantitatively, similar results were obtained in our separate calculation based on the tight-binding MO approximation in which infinite chain length of polypeptide is taken into account (T. Yamanobe, I. Ando, H. Saitō, R. Tabeta, A. Shoji, and T. Ozaki, *Mol. Phys.*, submitted for publication).
- (12) A. E. Tonelli and F. C. Schilling, *Acc. Chem. Res.*, **14**, 233 (1981).
- (13) A. E. Tonelli, *J. Am. Chem. Soc.*, **102**, 7635 (1980).
- (14) F. A. Bovey in "Proceedings of the International Symposium on Macromolecules, Rio de Janeiro, July 26–31, 1974, E. B.

- Mano, Ed., Elsevier, Amsterdam, 1975, p 169.
- (15) R. Ditchfield, D. P. Miller, and J. A. Pople, *J. Chem. Phys.*, **54**, 4186 (1971).
  - (16) M. Kondo, I. Ando, R. Chûjô, and A. Nishioka, *J. Magn. Reson.*, **24**, 315 (1976).
  - (17) I. Ando and T. Asakura, *Annu. Rept. NMR Spectrosc.*, **10A**, 81 (1980).
  - (18) K. A. K. Ebraheem and G. A. Webb, *Prog. Nucl. Magn. Reson. Spectrosc.*, **11**, 149 (1977).
  - (19) (a) I. Shavitt and M. Karplus, *J. Chem. Phys.*, **43**, 398 (1965); (b) C. W. Kern and M. Karplus, *ibid.*, **43**, 415 (1965).
  - (20) F. A. Momany, R. F. McGuire, J. F. Yan, and H. A. Scheraga, *J. Phys. Chem.*, **75**, 2286 (1971).
  - (21) S. Arnott and A. L. Wonacott, *J. Mol. Biol.*, **21**, 371 (1966).
  - (22) S. Arnott, S. D. Dover, and A. Elliot, *J. Mol. Biol.*, **30**, 201 (1967).
  - (23) K. Itoh, T. Nakahara, T. Shimanouchi, M. Oya, K. Uno, and Y. Iwakura, *Biopolymers*, **6**, 1759 (1968).
  - (24) Recently, we have observed that the  $C_\alpha$  and carbonyl  $^{13}C$  chemical shifts of the left-handed  $\alpha$ -helical poly( $\beta$ -benzyl-L-aspartate) (Asp(OBzl) $_n$ ), cast from chloroform solution and dried quickly, are very close to those of the  $\beta$ -sheet form, although the  $C_\beta$  signal is identical with that of the right-handed  $\alpha$ -helical (Asp(OBzl) $_n$ ). (H. Saito, R. Tabeta, I. Ando, T. Ozaki, and A. Shoji, *Chem. Lett.*, 1437 (1983).) This observation strongly supports our present assignment of the peaks i. As to the assignment of the peak i in the  $C_\beta$  carbon, one of the reviewers raised a question as follows. When a D-alanine adopts the  $\alpha_R$  helix its  $C_\beta$  carbon and carbonyl oxygen atoms are eclipsed, or cis. This overlapped arrangement of  $C_\beta$  is removed to L-alanine in the  $\alpha_R$ -helix. It is pointed out in ref 7 that this eclipsed arrangement is highly shielding and would be expected to result in the D-alanine  $C_\beta$  resonance appearing upfield from the  $C_\beta$  resonance in L-alanine ( $\alpha_R$ -helix). This view, however, is incorrect as viewed from the present experimental finding as well as that of (Asp(OBzl) $_n$ ). It is also emphasized that the variation of  $^{13}C$  chemical shifts, similar to that of (Ala) $_n$ , is well reproduced by a theoretical calculation (I. Ando et al., manuscript in preparation).
  - (25) F. A. Bovey in "Macromolecules, An Introduction to Polymer Science", F. A. Bovey and F. H. Winslow, Eds., Academic Press, New York, 1979, Chapter 8.

## Isotactic Polymerization of C-3 Branched $\alpha$ -Olefins: Conformation of the Monomer<sup>1</sup>

A. Zambelli,\* P. Ammendola, and A. J. Sivak<sup>2</sup>

Istituto Chimico dell'Università di Napoli, 80134 Naples, Italy. Received May 31, 1983

**ABSTRACT:** The rate constants of the initiation on metal-methyl bonds for isotactic polymerization of 3-methyl-1-pentene (3MP1), 3-methyl-1-butene (3MB1), and 3-ethyl-1-pentene (3EP1) have been compared to each other. Their relative values are accounted for by assuming that the monomers react with a possibly distorted H-skew or H-skew' conformation.

### 1. Introduction

In a previous paper it was pointed out that insertion of 3-methyl-1-pentene (3MP1) into the reactive metal-carbon bond of the active sites of Ziegler-Natta isotactic-specific catalysts is diastereoselective. It was actually observed that the  $R'R$  and  $S'S$  faces of the racemic monomer are twice as reactive as the  $S'R$  and  $R'S$  faces (Figure 1) both in the enantioselective chain propagation steps and in the nonenantioselective initiation on  $Mt-CH_3$  bonds.<sup>3,4</sup>

If one considers the most favored solution-state conformation of the olefin (H-syn)<sup>5-8</sup> (see Figure 2), it turns out that the more reactive faces of 3MP1 ( $R'R$  and  $S'S$ ) also appear to be the most hindered.

On the other hand, it is quite possible that the monomer is forced to achieve a different conformation in order to approach the reactive metal-carbon bond of the active site with a minimum of nonbonded interactions.

In this paper the reactivity of the diastereotopic faces of 3MP1 in the initiation on  $Mt-CH_3$  bonds is compared with the reactivity of the enantiotopic faces of 3-methyl-1-butene (3MB1) and 3-ethyl-1-pentene (3EP1). Some information concerning the conformation of the monomer in the active state is inferred.

### 2. Experimental Section

**Reagents.** 3MB1 was prepared according to the literature.<sup>9</sup> (RS)-3MP1 and 3EP1 were commercial products. The purity of the monomers was checked by GLC (>98%). The monomers and the polymerization diluent (pentane) were distilled under vacuum in the presence of a small amount of  $Al(n-C_4H_9)_3$  just before polymerization.  $^{13}C$ -enriched (34%)  $Al(CH_3)_3$  and  $Zn(CH_3)_2$  were prepared according to ref 10.  $\delta-TiCl_3$  was prepared according to the literature<sup>11</sup> (elemental analysis: Ti, 20.18; Al, 7.45; Cl, 69.60).

**Copolymerization of 3MB1 and (RS)-3MP1.** Five milliliters of anhydrous pentane,  $4.9 \times 10^{-3}$  mol of  $\delta-TiCl_3$ ,  $1.2 \times 10^{-3}$  mol of  $Al(^{13}CH_3)_3$ , and  $2.9 \times 10^{-3}$  mol of  $Zn(^{13}CH_3)_2$  were introduced under nitrogen into a 60-mL reactor provided with a magnetic stirring bar and cooled to  $-78^\circ C$ . The reactor was then cooled with liquid nitrogen and evacuated with a diffusion pump. Next,  $1.2 \times 10^{-1}$  mol of (RS)-3MP1 and  $2.6 \times 10^{-2}$  mol of 3MB1 were condensed into the reactor through a vacuum line. The reactor was transferred into a thermostated bath. After 5 h of stirring at  $50^\circ C$  the polymerization was stopped by injecting 5 mL of 2-ethylhexanol into the reactor. Polymer yield was 0.65 g.

**Copolymerization of 3EP1 and (RS)-3MP1.** The copolymerization was performed as above, with 5 mL of pentane,  $6 \times 10^{-3}$  mol of  $\delta-TiCl_3$ ,  $1.3 \times 10^{-3}$  mol of  $Al(^{13}CH_3)_3$ ,  $3.1 \times 10^{-3}$  mol of  $Zn(^{13}CH_3)_2$ ,  $6.2 \times 10^{-2}$  mol of (RS)-3MP1, and  $9.2 \times 10^{-2}$  mol of 3EP1. Polymerization time was 20 h; yield was 0.4 g.

**Fractionation.** The copolymers were fractionated by subsequent exhaustive extractions with boiling diethyl ether and toluene.<sup>12</sup> The results are reported in Table I.

**$^{13}C$  NMR Analysis.** Proton-noise-decoupled  $^{13}C$  NMR analysis of the samples dissolved in 1,2,4-trichlorobenzene containing 20% tetrachloroethane-1,2- $d_2$  for field-frequency stabilization and HMDS as an internal standard was carried out at  $130^\circ C$  in the PFT mode on a Varian XL-200 spectrometer operating at 50.309 MHz. Pulse width was 4.7  $\mu s$ . The fractions insoluble in boiling toluene were thermally degraded as described in ref 3.

**X-ray Analysis.** X-ray spectra of unoriented samples were obtained with a Philips APD spectrometer using  $Cu K\alpha$  radiation. Both the toluene-soluble fractions and the toluene-insoluble fractions were found to have nearly the same degree of crystallinity.

### 3. Results

(RS)-3MP1 has been copolymerized with 3MB1 or 3EP1 in the presence of the isotactic-specific catalytic system